

## 4. MEASUREMENT SYSTEM AND PROCEDURES

The purpose of this section is to provide a detailed summary of the measurement system, test procedures, GPS-receiver and UWB-signal sample space, signal generation details, and hardware limitations for this experiment.

### 4.1 System

The GPS interference test bed utilized in this experiment was developed at ITS (see Figure 4.1.1). It is comprised of three segments – GPS source, UWB source, and GPS receiver. System configuration is illustrated in Figure 4.1.2 and hardware components are specified in Table 4.1.1 and Appendix B. Each of the contributing signals (i.e., GPS, noise, and UWB) were filtered, amplified, and combined prior to input into the receiver. Signal powers were controlled using precision variable attenuators (VA) controlled by computer. The following subsections provide signal-generation details and justification for hardware employed.

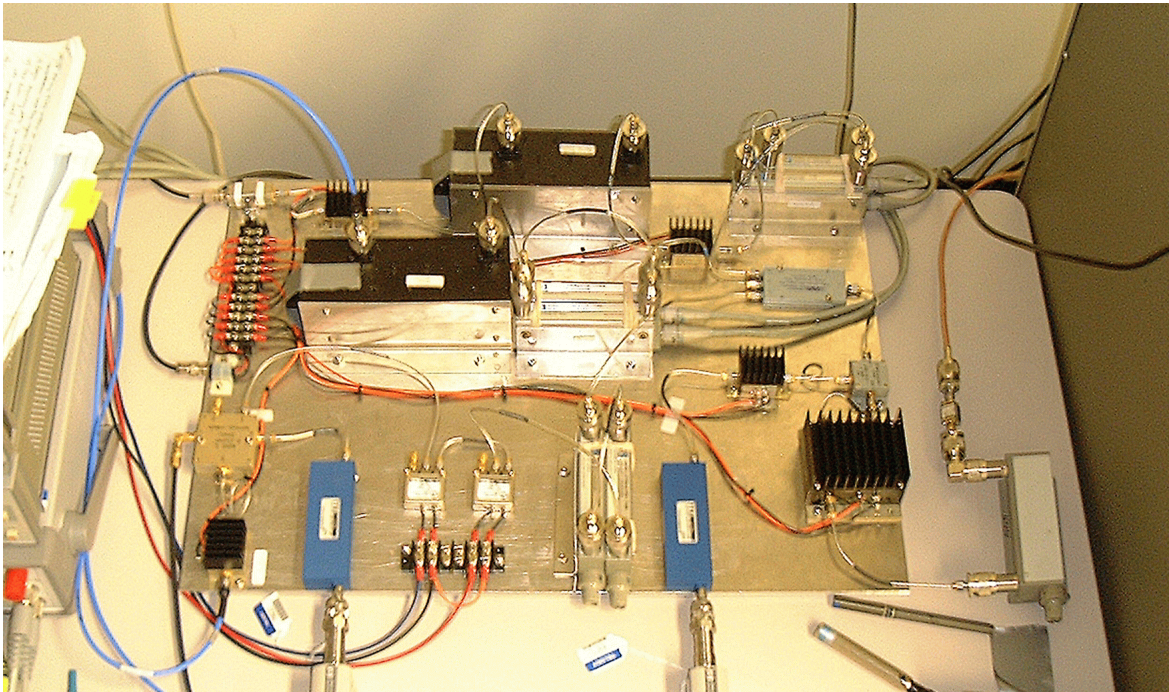


Figure 4.1.1. GPS Interference test bed.

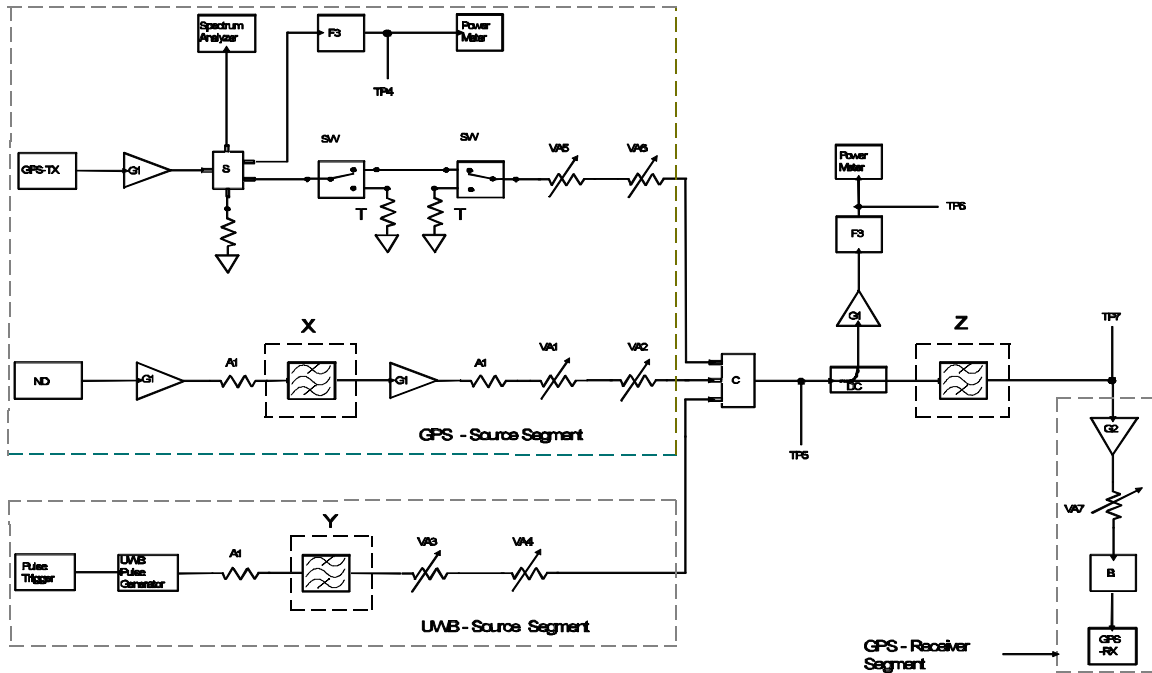


Figure 4.1.2. Block diagram.

Table 4.1.1. Variations in Configuration for Different Receivers

Receiver Description (Rx #)	Noise Diode	Injected Noise <sup>1</sup> (dBm/20MHz)	Fixture <sup>2</sup> X	Fixture Y	Fixture Z
C/A Code (Rx 1)	ND1	-93	F1	F1	Bypassed
Semi-Codeless (Rx 2)	ND2	-120	F2	F2	F4/A2

<sup>1</sup> Gaussian noise power density (dBm/20 MHz) at point TP7 on the test fixture.

<sup>2</sup> Fixtures X, Y, and Z are shown in Figure 4.1.2, and part number are described in Appendix B

#### 4.1.1 GPS-Source Segment

The purpose of the GPS segment is to provide a simulated GPS signal at a known SNR. The GPS signal and background noise were generated with a multi-channel GPS simulator (GPS-TX) and a noise diode (ND), respectively.

Utilization of a GPS simulator provides high-accuracy repetition of scenarios and flexibility for simulation over a wide range of normal and abnormal situations. Generated GPS signals appear as though they had been transmitted from multiple moving satellites, and the simulated satellite positions can be reset to a selected standard configuration at the beginning of each test. Simulated navigation data, required by the user segment and contained in the GPS spread spectrum signal, consists of satellite clock, ephemeris (precise satellite position), and almanac (course satellite position) information.

The GPS simulator used in this experiment is the Nortel model STR2760 provided by the 746<sup>th</sup> Test Squadron at Holloman Air Force Base. It is the responsibility of the 746<sup>th</sup> Test Squadron to verify simulator integrity and consistency by comparing simulated signals to measured data; the STR2760 has met those requirements. It reproduces the environment of a GPS receiver installed on a dynamic platform and accounts for receiver and satellite motion and atmospheric effects (e.g., ionospheric delay, tropospheric attenuation and delay, and multipath).

The receiver location was chosen as 32EN, 106EW, and 1000 m above sea level, and the 75-minute scenario was based on an actual constellation beginning on December 16, 1999 at 9:30 p.m. The simulated signals contain Doppler shifts and variable path lengths through the atmosphere according to satellite motion and elevation angle, respectively. Tropospheric attenuation and multipath were turned off. Also, ionospheric delay was simulated only for the receiver with dual-frequency cross-correlation capability.

In this experiment, we focus on the effects of imposed interference. The minimum number of satellites for a receiver to operate nominally, typically four, was chosen. Satellite geometry during the course of the simulation, shown in Figure 4.1.1.1, produces a Position Dilution-of-Precision (PDOP) between 2 and 3. Space vehicle (SV) 25 was chosen as the focus of the experiment. The transmitted signal powers of the other satellites were set to 5 dB greater than that of SV 25. Therefore, under the same interference conditions the SV-25 SNR will be significantly less than the other satellites, and performance degradation will be isolated to the SV-25 channel. Most importantly, as interference is increased the receiver will lose lock on SV 25 first.

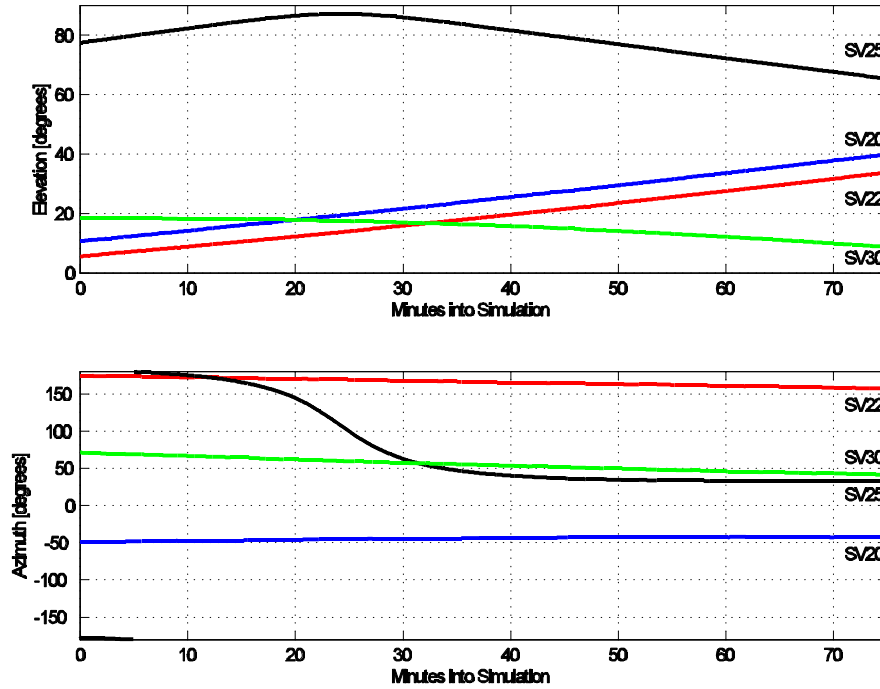


Figure 4.1.1.1. Simulated satellite geometry.

GPS is a CDMA system where multiple transmitters share the same bandwidth. Elevated co-channel interference present with some satellite combinations can produce GPS signal outages. This co-channel interference is approximated with Gaussian noise and emulated with a noise diode in the GPS segment.

#### 4.1.2 UWB-Source Segment

The UWB segment consists of a narrow-pulse generator and a triggering device to create various signals. The pulse shape/width, as a characteristic of the pulse generator, determines the overall spectral envelope. The manner in which the pulses are sequentially spaced (set by the triggering device) determines spectral content within the confines of the envelope. For instance, uniformly spacing the pulses creates strong spectral lines. Dithering the pulse spacing, however, reduces spectral line amplitude and increases noise power density.

The primary criterion for choosing a UWB pulse generator for these measurements depended on whether the spectral envelope was flat and produced sufficient power across the L1 and L2 bands. Two types of UWB pulse generators were utilized, one with a pulse width of 245 ps, and the other with a pulse width of 500 ps. Descriptions of the pulse generators are provided in greater detail in Appendix B. Both pulse generators are triggered by an external device (e.g., arbitrary waveform generator, custom built triggering circuit) to produce different sequential pulse spacings.

For these measurements, the UWB signal is specified by a combination of pulse repetition frequency (PRF), mode of spacing, and the application of gating, all of which have distinctly different effects on spectral and time domain characteristics of the signal.

Four distinct modes of spacing were used: uniform pulse spacing (UPS), on-off keying (OOK), absolute (clock) referenced dithering (ARD), and relative (clock) referenced dithering (RRD). The vertical dashed lines in Figure 4.1.2.1 represent the ticks of a clock. UPS, as the name implies, is a pulse train of equal spacing, where pulses occur at the clock ticks. OOK refers to the process of selectively “turning off” or eliminating pulses at the clock ticks. ARD produces pulses that are dithered in relation to the clock tick. RRD dithers each pulse in relation to the previous pulse position.

The PRF for UPS, OOK, and ARD is equal to the clock rate; for our purposes, the PRF of RRD is defined as the reciprocal of the mean pulse interval. The extent of dither is expressed in terms of the percentage of pulse repetition period, which is the reciprocal of PRF.

Gating refers to the process of distributing pulses in bursts. This is represented in Figure 4.1.2.1 by the removal of the pulses in the shaded areas; in the case of the UPS example, there are 4 pulses generated during the gated-on time followed by 8 clock ticks for which there are no pulses (to give a duty cycle of 33%).

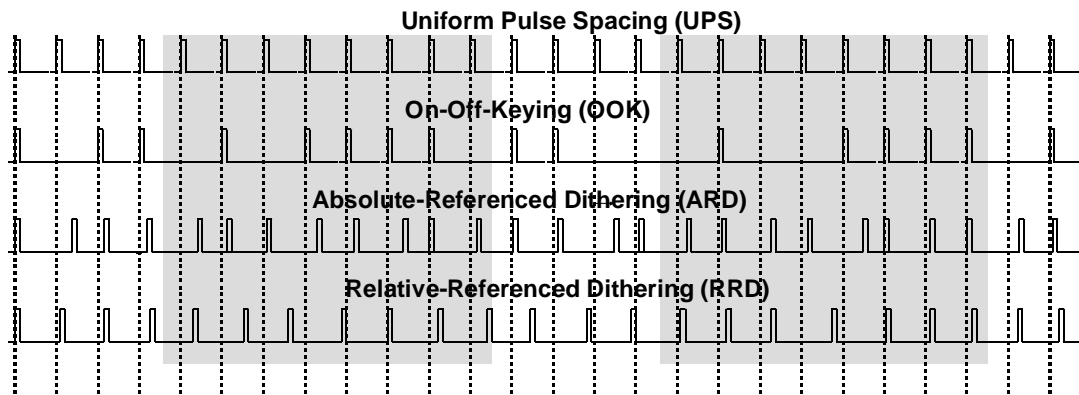


Figure 4.1.2.1. Pulse spacing modes.

## UWB Signal Space

By varying the three parameters – PRF, pulse spacing, and gating – 32 different permutations were chosen to span the full range of existing and potential UWB signals. For these measurements (as shown in Table 4.1.2.1) there are four PRFs (i.e., 0.1, 1, 5, and 20 MHz), four pulse spacing modes (i.e., UPS, OOK, 50% ARD, and 2% RRD), and two

gating scenarios (i.e., no gating and 20% gating with a 4 ms on-time). In addition, various combinations of UWB signals were summed to produce aggregate signals as shown in Table 4.1.2.2.

Table 4.1.2.1. UWB Signal Space

UWB Signal Parameter	Range
Average Power Density	As needed to induce effect on GPS receiver.
Pulse Width	0.245 and 0.5 nanoseconds
Pulse Repetition Frequency	0.1, 1, 5, 20 MHz
Modulation, Dithering	UPS, OOK, 50%-ARD, 2%-RRD
Gating	100% (no gating) and 20% Duty Cycle

Table 4.1.2.2. Aggregate UWB Signal Space

Aggregate	UWB Signal Parameters
1	6 × 10-MHz PRF, 2%-RRD, Non-Gated
2	6 × 10-MHz PRF, 2%-RRD, Gated (20% Duty Cycle)
3	2 × 10-MHz PRF, UPS, Non-Gated 1 × 3-MHz PRF, UPS, Non-Gated 3 × 3-MHz PRF, 2%-RRD, Gated (20% Duty Cycle)
4	3 × 3-MHz PRF, UPS, Gated (20% Duty Cycle) 3 × 3-MHz PRF, 2%-RRD, Gated (20% Duty Cycle)
5	(a) 1 × 1-MHz PRF, 2%-RRD, Non-Gated (b) 2 × 1-MHz PRF, 2%-RRD, Non-Gated (c) 3 × 1-MHz PRF, 2%-RRD, Non-Gated (d) 4 × 1-MHz PRF, 2%-RRD, Non-Gated (e) 5 × 1-MHz PRF, 2%-RRD, Non-Gated (f) 6 × 1-MHz PRF, 2%-RRD, Non-Gated

## Spectral Considerations

Spectral plots are shown in Figure 4.1.2.2 for four different UWB signals as they are passed through an L1 bandpass filter. UPS has the power gathered up into spectral lines at intervals of PRF. The greater the PRF, the wider the line spacing, and the greater the power contained in each spectral line. OOK also has spectral lines spaced at intervals of PRF that are superimposed on continuous noise-like spectrum. Dithered signals have spectral

characteristics inherently different from either UPS or OOK. For these measurements, ARD has a pulse spacing that is varied by 50% of the referenced clock period. RRD has a pulse spacing that is varied by 2% of the average pulse period. Both of these dithered cases have spectral features that are characteristic of noise (i.e., no spectral lines).

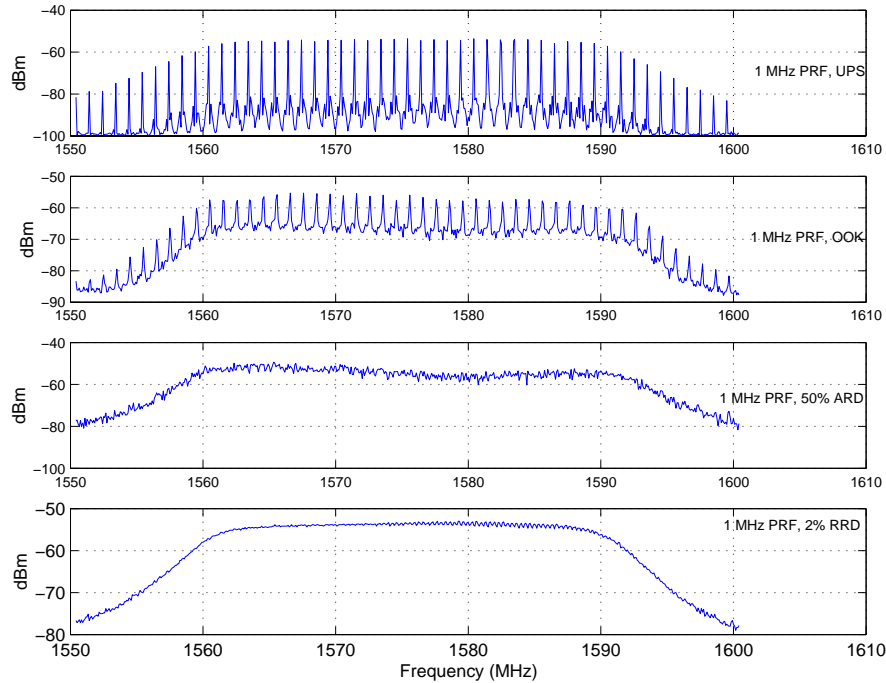


Figure 4.1.2.2. Spectral characteristics of the different pulse spacing modes.

Another feature worth noting is the phenomenon of spectral lines spreading due to gating. The spectrum of the gated UWB signal is the result of convolving the non-gated spectrum with the Fourier transform of the gating signal, which for our purposes is a  $\text{sinc}^2$  envelope. It follows that the single line of the non-gated cases is spread out into a multitude of lines confined by the  $\text{sinc}^2$  envelope, where the spacing between lines, or line spread spacing (LSS), is equal to the reciprocal of the gating period; null spacing, or line spreading null-to-null bandwidth (LSNB), of the main lobe of the  $\text{sinc}^2$  function is equal to two times the reciprocal of gated-on time.

There are two additional spectral features that occur as a result of the signals having been generated by an arbitrary waveform generator (AWG). One is related to how the pattern of pulses is repeated, and the other has to do with the process of placing the pulses into bins, representing discrete dithered pulse spacing. Further discussion of these spectral characteristics of UWB signals is contained in Appendix C.

## Spectral Line Alignment

Because each of the emulated satellites is mobile in nature, there is a corresponding Doppler shift associated with its motion and direction. Figure 4.1.2.3 shows the emulated Doppler frequency for SV 25 going from the beginning to the end of the simulation. Notice that the C/A code lines shift nearly 2.25 kHz over the course of the simulation. For those UWB signals which contain spectral lines, alignment of the UWB spectral lines and the SV-25 spectral lines over a period of 40 minutes is inevitable. To assure controlled measurement conditions, both the GPS simulator and the AWG were time referenced with the same rubidium oscillator and the spectral lines of the UWB signals were precisely placed, as described in detail in Appendix C, Table C.1.1. Figure 4.1.2.4 illustrates the manner in which these spectral lines were placed. Because SV 25 has a particularly vulnerable spectral line at 1575.571000 MHz, each of the UWB signals with discrete spectral lines were created with a spectral line at 1575.570571 MHz – approximately half way between GPS spectral lines. As described in Section 4.3, data acquisition started at 20 minutes into the simulation (at approximately 0 Hz Doppler shift) and continued for the next 20 minutes; hence, spectral alignment was guaranteed.

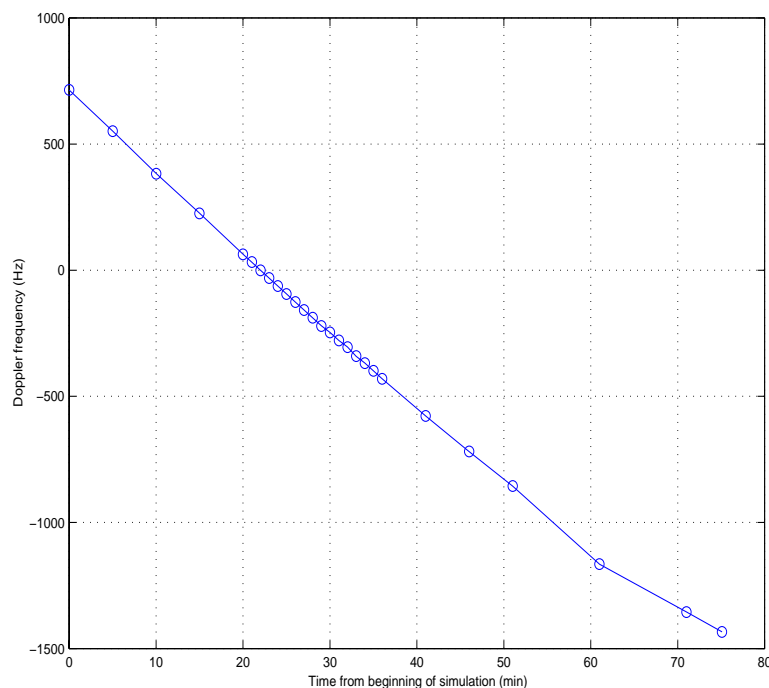


Figure 4.1.2.3. Doppler frequency of SV25.



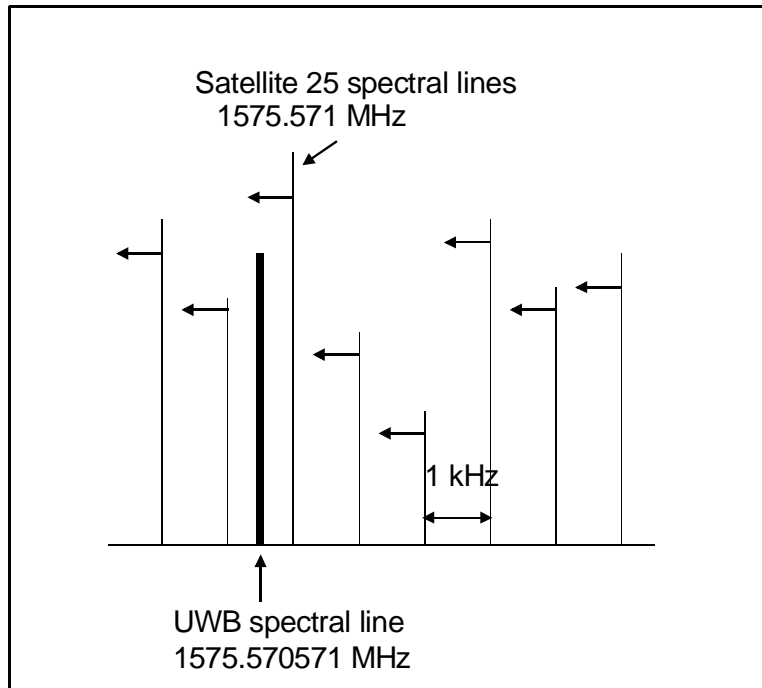


Figure 4.1.2.4. Spectral line placement.

### 4.1.3 GPS-Receiver Segment

The typical stand-alone GPS receiver is implemented on specialized ASICs and DSP chips. The information from GPS signals is processed, according to proprietary adaptive algorithms, to meet design specifications for specific applications. For example, navigational receivers require reliable position information and fast recovery from outages, while surveying receivers require high-precision position accuracy. Each receiver may generate different failure modes from interference and may recover from interference in different ways.

Two receivers encompassing different technologies were selected and are given in Table 4.1.1. These receivers employ various techniques to accomplish their individual design specifications. As a rule of thumb, the receivers under test were left at their factory default settings with two exceptions. First, stand-alone mode was always specified; that is, DGPS, pseudolites, and external sensors (e.g., altimeters, inertial navigation equipment) were disabled. Secondly, carrier smoothing was removed whenever possible in order to minimize the number of correlated data points. Appendix B provides a table of settings for each receiver.

Each receiver has an active antenna with a specific gain and bandwidth. Because the conducted measurements bypassed the antenna, input signals were filtered and amplified to give an equivalent bandwidth and gain of the respective receiver antenna. A preselection filter and low noise amplifier (LNA) were placed in front of the receiver for the purpose of

matching, as close as possible, the filter and amplifier characteristics of the antenna unit. Receiver 2, however, required an active L1/L2 filter with a 27-MHz bandwidth which is approximately half the bandwidth of the accompanying antenna.

It is assumed that the receiver bandwidth sets the narrowest bandwidth for signal path, and therefore, the equivalent antenna bandwidth filter is not critical to the outcome of the results. This was verified by measurements using two different equivalent antenna bandwidths for the same receiver. However, for practical purposes, the preselector filters were also used to prevent saturation of amplifiers utilized in the test fixture. The discussion on radiated versus conducted measurements, given in Appendix A, is also relevant to this topic.

## 4.2 Power Measures, Settings, and Calibration

The purpose of this section is to clarify power measurement terminology, discuss power level settings of the various signal sources, and describe the calibration procedures used to assure the proper power levels.

### 4.2.1 Carrier-to-Noise Density Ratio Settings

To account for other potential sources of interference, such as sky noise, cross-correlation noise from other satellites within the GPS constellation, and GPS augmentation systems, broadband noise was added to the GPS-source segment. The level of broadband noise – based on minimum  $C/N_0$  requirement for acquisition of a GPS satellite – was set to 34 dB-Hz [3]. Based on the minimum guaranteed GPS signal power ( $C$ ) specification for the C/A code of -130 dBm into a 0 dBic gain antenna [4] and a 2 dB implementation loss ( $L_{imp}$ )<sup>1</sup> the maximum broadband noise density level at which satellite acquisition can be ensured is:

$$N_0 = C - L_{imp} - C/N_0 = -130 - 2 - 34 = -166 \text{ dBm/Hz.}$$

Because the broadband noise was measured at the output of a 20-MHz bandpass filter, the added-noise power level is then calculated as:

$$N = -166 + 10 \log (20 \times 10^6) = -93 \text{ dBm/20 MHz.}$$

The use of a broadband noise level based upon the  $C/N_0$  acquisition threshold is supported by computer simulations performed within the International Telecommunication Union Radiocommunications Sector (ITU-R). The simulations in ITU-R Recommendation M.1477 show how  $C/N_0$  can vary over a 24-hour period, at different user locations, when only sky

---

<sup>1</sup> The implementation loss takes into account the loss due to IF filtering, the loss due to the analog-to-digital conversion, correlation loss due to modulation imperfections in the GPS signal and other miscellaneous losses.

noise and GPS cross-correlation noise are considered. The results of this simulation indicate that without any additional interference from external sources, and under certain worst case conditions, the  $C/N_0$  level can fluctuate to within 1 dB of the acquisition threshold of 34 dB-Hz.

#### 4.2.2 Calibration and Power Level Correction

For these measurements, all signal powers were measured with a power meter and expressed as a mean value. Wideband sources, such as UWB signals and noise, are expressed in terms of power density in a 20-MHz bandwidth (centered at 1575.42 MHz). This section describes the various steps taken to assure power-level accuracy.

To assure that no test-fixture amplifier became saturated throughout the measurements and verify functionality, power levels were measured throughout the test fixture using the full range of signals and power levels. Amplifiers, in addition, were tested for linearity – also using the full range of signals and power levels.

Prior to every interference measurement, power levels of the GPS, noise, and UWB signals were measured without attenuation imposed. Measured power at TP4 and TP6 (in Figure 4.1.2) are referenced to the input of the LNA (TP7) via calibration factors which account for the losses associated with individual power-measurement paths. During the test, contributing power levels were determined by subtracting an applied attenuation from the respective 0-dB attenuation measurements. Additionally, each attenuator was checked for integrity before each test.

Because noise was measured in a bandpass filter centered at the L1 frequency, and because some power passed through the filter outside the 20-MHz bandwidth, a power correction was applied. This correction factor was determined by passing the noise through the filter and measuring the noise power with a spectrum analyzer over a range of frequencies centered at 1575.42 MHz. The power was integrated over 100 MHz and then integrated again across 20 MHz. The difference between these two values (in dB) is subtracted from the measured noise power, giving a spectral power density in the 20 MHz bandwidth.

To assure proper and consistent power levels at the output of the GPS simulator, the GPS signal power of SV 25 was measured at the beginning of each test. All other satellites were turned off during power measurement. To reduce the noise contribution and exclude the L2 signal, the power was measured through an L1 bandpass filter centered at 1575.42 MHz; however, because the power meter measures both the C/A and P code, a calibration factor was applied to determine the power of the C/A code only. This calibration factor was determined by measuring and theoretically verifying the difference in power levels between having only the C/A code turned on and having both the P and C/A codes turned on.

Two other issues regarding power settings has to do with measuring and setting the power of gated and aggregate signals. Because the power meter does not accurately measure gated signal powers, all gated signal powers were measured without gating. As mentioned earlier, the power of all gated signals, used during interference measurements, is expressed as the average power of the non-gated signal. Twenty percent gating reduces mean non-gated signal power by 7 dB. Finally, all signals contributing to the aggregate signals shown in Table 4.1.2.2 have equal peak powers.

### **4.3 Measurement Procedure**

In this experiment, two separate tests were performed to measure break-lock and reacquisition-time behavior (flowcharts are given in Figures 4.3.1 and 4.3.2, respectively). The procedures were implemented in software to enhance repeatability, automate testing, and provide a vehicle for extracting information from the receivers.

During RQT measurements, the GPS simulator used a dynamic scenario emulating a mobile receiver traveling at 10 m/s. During BL measurements, a static scenario was used. The measurements were delayed 20 minutes every time the simulator was reset. This twenty-minute delay is based on the fact that it takes a minimum of 12.5 minutes for the receiver to download the entire navigation message from the constellation; hence, we assume 20 minutes is enough time for the almanac/ephemeris data inside the receiver to be up-to-date and complete.

The basic BL measurement consists of turning off interference, reestablishing lock, turning on interference, and sampling the receiver's loss-of-lock indicator once per second over the BL measurement duration (approximately 17 minutes). The BL test shown in Figure 4.3.1 determines the BL point. This is accomplished by incrementing UWB signal power by 3 dB between BL measurements until BL occurs. The BL test then decrements the UWB signal power in 1-dB steps until lock is maintained continuously over the entire measurement duration. The BL point is defined as 1 dB above this final UWB signal power. During BL measurements, the following observational parameters were sampled once per second for data analysis: pseudorange, observation time, clock offset, carrier phase, Doppler frequency shift, signal-to-noise ratio, potential cycle slip, position data, and receiver tracking status.

The basic RQT measurement consists of turning off the zenith satellite, setting the interference level, delaying 10 seconds, turning on the zenith satellite, applying the interference, and measuring the number of seconds until the receiver achieves lock. A RQT measurement is successful if lock is achieved within 2 minutes and maintained for at least 1 minute. The RQT test summarized by the flowchart in Figure 4.3.2 is performed by incrementing UWB signal power by 3 dB between sets of 10 RQT measurements. The test is complete when all 10 RQT measurements at a single UWB power are unsuccessful.

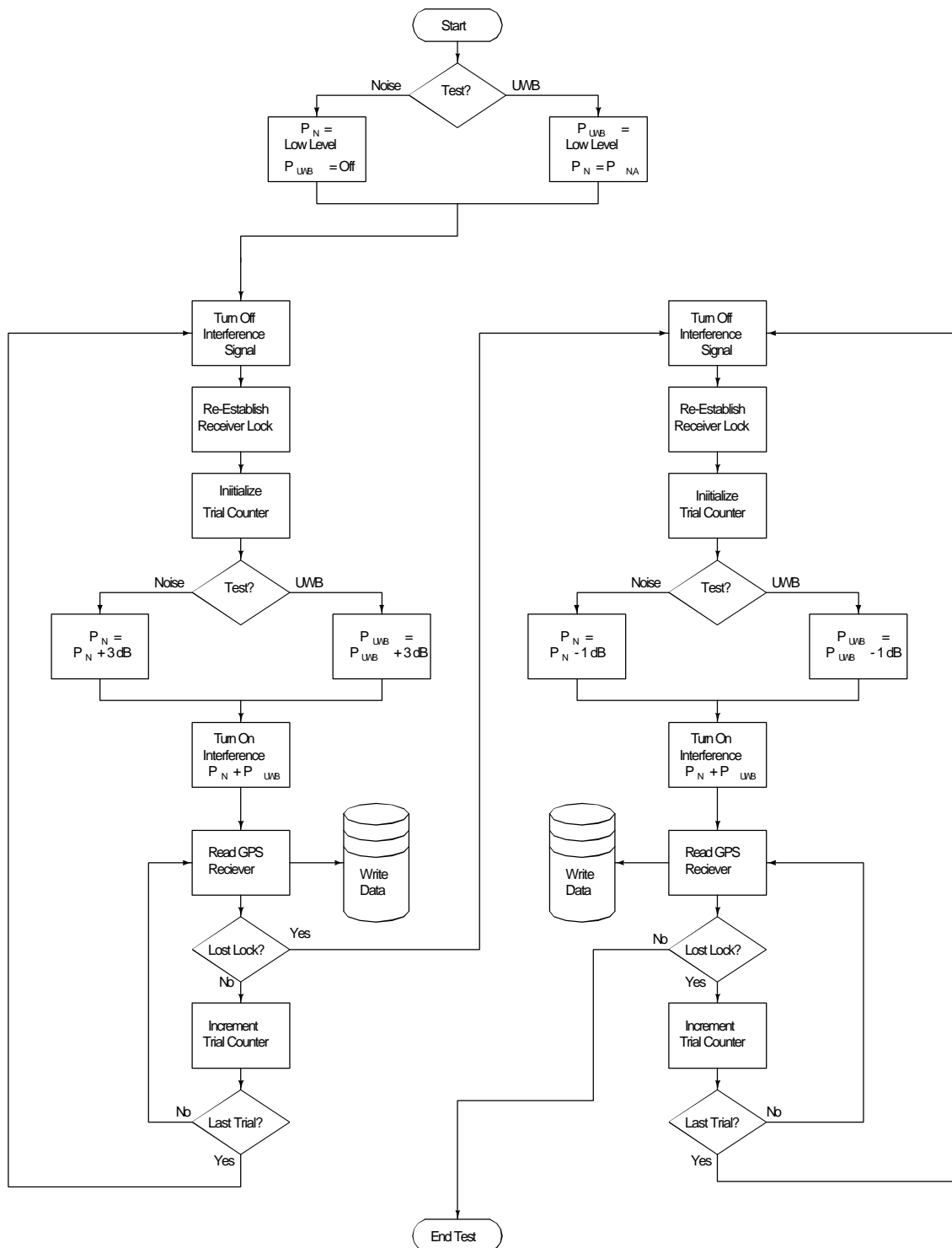


Figure 4.3.1. Break-lock test flowchart.

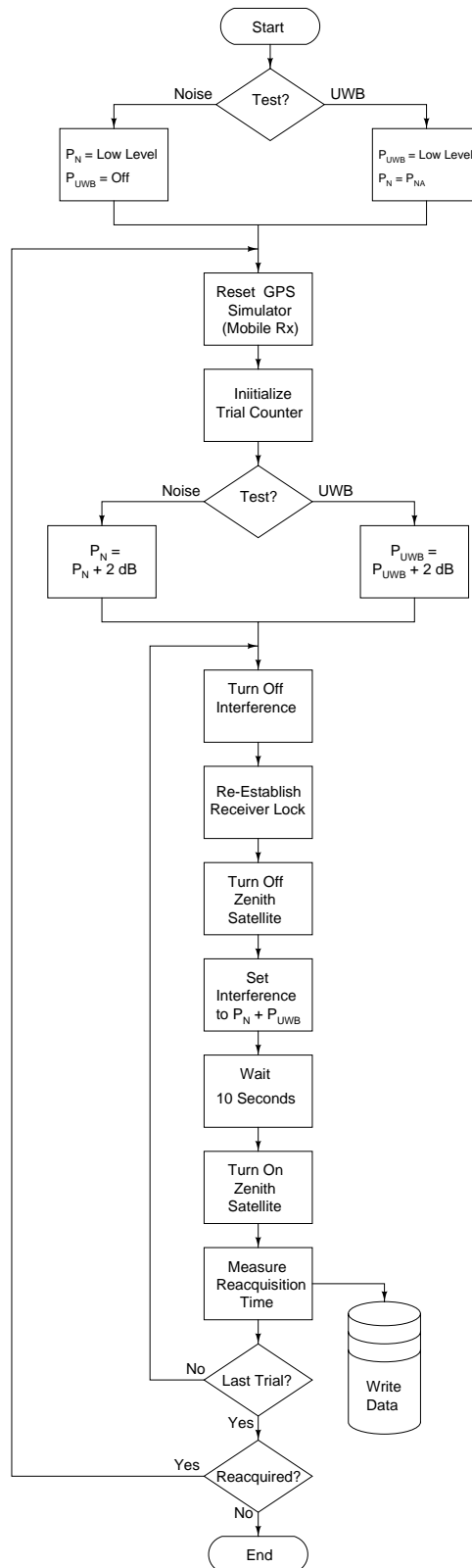


Figure 4.3.2. RQT test flowchart.